
Audiovisual Speech Synthesis using Tacotron2

Ahmed Hussen Abdelaziz*
Apple
Cupertino, CA
ahussenabdelaziz@apple.com

Anushree Prasanna Kumar*
Apple
Cupertino, CA
ak_26@apple.com

Chloe Seivwright
Apple
London
cseivwright@apple.com

Gabriele Fanelli
Apple
Zurich
gabriele_fanelli@apple.com

Justin Binder
Apple
Cupertino, CA
jbinder@apple.com

Yannis Stylianou
Apple
London
istylianou@apple.com

Sachin Kajarekar
Apple
Cupertino, CA
skajarekar@apple.com*

Abstract

Audiovisual speech synthesis is the problem of synthesizing a talking face while maximizing the coherency of the acoustic and visual speech. In this paper, we propose and compare two audiovisual speech synthesis systems for 3D face models. The first system is the AVTacotron2, which is an end-to-end text-to-audiovisual speech synthesizer based on the Tacotron2 architecture. AVTacotron2 converts a sequence of phonemes representing the sentence to synthesize into a sequence of acoustic features and the corresponding controllers of a face model. The output acoustic features are used to condition a WaveRNN to reconstruct the speech waveform, and the output facial controllers are used to generate the corresponding video of the talking face. The second audiovisual speech synthesis system is modular, where acoustic speech is synthesized from text using the traditional Tacotron2. The reconstructed acoustic speech signal is then used to drive the facial controls of the face model using an independently trained audio-to-facial-animation neural network. We further condition both the end-to-end and modular approaches on emotion embeddings that encode the required prosody to generate emotional audiovisual speech. We analyze the performance of the two systems and compare them to the ground truth videos using subjective evaluation tests. The end-to-end and modular systems are able to synthesize close to human-like audiovisual speech with mean opinion scores (MOS) of 4.1 and 3.9, respectively, compared to a MOS of 4.1 for the ground truth generated from professionally recorded videos. While the end-to-end system gives a better overall quality, the modular approach is more flexible and the quality of acoustic speech and visual speech synthesis is almost independent of each other.

Keywords: Audiovisual speech, speech synthesis, Tacotron2, emotional speech synthesis, blend-shape coefficients

*Ahmed H. Abdelaziz and Anushree P. Kumar have contributed equally

1 Introduction

Human perception of speech is inherently bimodal (audiovisual). In face-to-face conversations, vision improves the intelligibility of speech by reading the lips of the talker. Such forms of visual hearing are exploited not only by hearing impaired people, but also by all individuals [10]. The presumed biological link between perception and production makes bimodal speech production essential in generating realistic talking characters. Thus, audiovisual speech synthesis involves synthesizing visual controllers for a face model that is coherent with the synthesized acoustic speech units. This is extremely challenging, as we, humans, are highly sensitive to any subtle alteration or poor synchronization between lip movements (visual speech) and accompanied acoustic speech. Poor visual speech synthesis can negatively influence the intelligibility of what is being spoken [22] even if the accompanied synthesized acoustic speech is relatively natural. Additionally, since the same speech units can be uttered in different ways depending on the underlying facial expressions, it becomes essential to synthesize plausible facial expressions along with acoustic speech and lip movements to increase the naturalness of visual speech synthesis.

Recent advances in neural text-to-speech (TTS) systems have led to synthesizing close-to-human-like speech. One of the widely used neural TTS architectures is Tacotron 2 [26]. In this paper, we describe two approaches for audiovisual speech synthesis using this model. The first one, which we call AVTacotron2, is an end-to-end approach, where facial controls along with the speech’s spectral features are synthesized directly from text. The resulting spectral features are then used to reconstruct the speech signal using WaveRNN [17]. The facial controllers generated by the AVTacotron2 are used to animate a 3D face model. Finally, the video of the talking face is generated by combining the synthesized acoustic and visual information. The second approach is modular, where we use the Tacotron2 system in a regular fashion to synthesize acoustic speech from text. Then, we use an independent speech-to-animation module that generates the corresponding facial controls from the synthesized speech. Speech signal reconstruction and video generation are done in the same way as in the end-to-end approach.

Both the end-to-end and modular systems preserve the synergy between the synthesized acoustic and visual speech. Also, both approaches synthesize talking faces that can be directly deployed in computer graphics applications, such as computer-generated movies, video games, video conferencing, and virtual agents in virtual and augmented reality, without any manual post-processing. The modular approach provides more flexibility, as the audio-to-animation module can be easily trained to generalize across many speakers [1]. It can then be conveniently used with any voice and/or language synthesized by any text-to-speech system. Also, the quality of the acoustic and visual speech is almost decoupled. This means each of the modules can be optimized separately without compromising the quality of the other module. On the other hand, the end-to-end solution consists of a single neural network that automatically captures the correlation between the audio and visual cues. Our results show that it also gives better overall synthesis quality compared to the modular system.

In this work, we represent the space of facial motion using generic blendshapes. The benefit of using such a facial representation is twofold: 1) It provides a semantic meaning of the facial controls, i.e., the blendshape coefficients, which makes them easy to analyze and post-process for further improvements. 2) The blendshape coefficients can be applied to a variety of fictional and human-like face models.

Synthesizing human-like audiovisual speech is more complicated than just producing raw acoustic and visual speech. Modulating the synthesized speech with the corresponding prosody [28] and facial expressions is a crucial quality factor for audiovisual speech synthesis. Recently, many significant breakthroughs in style modeling have been proposed in the speech synthesis realm [38]. In this study, we are addressing the synthesis of easy-to-define styles of speech, which are emotions. We present a supervised approach for emotion-aware audiovisual speech synthesis. In particular, we condition both the end-to-end and modular approaches on emotion embeddings that encode the required prosody of audiovisual emotional speech. The emotion embeddings are extracted from a stand alone speech emotion classifier.

Evaluating audio-only and audiovisual speech synthesis systems is challenging, as their quality need to be assessed using human perception. In this paper, we evaluate the two proposed systems using various subjective tests. Different tests focus on different aspects of the synthesis, such as acoustic

speech quality, lip movement quality, facial expression, and emotion in speech. We use mean opinion score (MOS) tests as well as AB tests to obtain absolute and relative scores for the two approaches. We also evaluate the holistic perception of the talking face.

To summarize, the main contributions of this study are:

- We describe and evaluate two systems for emotion-aware audiovisual speech synthesis based on Tacotron2: an end-to-end (AVTacotron2) and a modular approach. We show that both systems generate close to human-like emotional audiovisual speech without requiring post-processing.
- We apply these approaches to a generic blendshape model that allows for synthesizing a variety of 3D face models.
- The definition of empirical evaluation tests that assess the quality of different aspects of the synthesized speech as well as the overall quality. We compare the synthesis quality of the proposed systems to the original recordings of a professional actress.

The rest of the paper is organized as follows: In Section 2, we discuss the related work. Section 3 describes the problem of the offline extraction of facial controls from video sequences. In Section 4, we introduce the speech emotion recognition system used for extracting emotion embeddings. Section 5 outlines the model architectures of the end-to-end approach for synthesizing audiovisual speech from text. The modular approach is then described in Section 6. The experiments used to evaluate the model performance and the results are described in Section 7. Finally, we conclude the paper and give an outline of future work in Section 8.

2 Related work

Manually and Video-driven Avatars: Although there has been an increasing trend in sophisticated face and motion tracking systems, the cost of production still remains high. In many production houses today, high fidelity speech animation is either created manually by an animator or using facial motion capture of human actors [4, 6, 14, 40, 42]. Both manually and performance-driven approaches require a skilled animator to precisely edit the resulting complex animation parameters. Such approaches are extremely time consuming and expensive, especially in applications such as computer generated movies, digital game production, and video conferencing, where talking faces for tens of hours of dialogue are required. To solve this problem, speech- and text-driven talking faces can be used. In this study, we introduce new text-driven approaches for synthesizing production-quality speech and facial animation with different styles of speech.

Face Representations: Face synthesis algorithms can be categorized into two major categories: photorealistic and parametric. In photorealistic synthesis, videos of the speakers are generated either from text or audio inputs [20, 29, 34]. These techniques involve combining both image and speech synthesis tasks.

In parametric face synthesis, a sequence of facial controllers are used to deform a neutral face model. The parametric approaches can either operate on 3D face models [3, 7] or on 2D images. For the 2D face synthesis, active appearance models (AAMs) [9] are widely used. In this technique, a face is modeled using shape and appearance parameters. However, due to modeling non-linear variability by a linear PCA model and the low rank approximations, details such as the regions near the mouth often appear blurry [12].

Our approach belongs to the parametric synthesis category, where a sequence of low-dimensional blendshape coefficient vectors are synthesized and applied to a wide range of 3D avatars. We use a method similar to that in [39] for offline extraction of the ground truth blendshape coefficients, which are used as facial controllers for the 3D face model.

Text-driven Avatars: Many approaches have been proposed for visual and audiovisual speech synthesis from text. For visual speech synthesis, hidden Markov models (HMM) were used in earlier approaches, e.g., in [13, 25, 36, 41]. In [25] and [36], HMM-based systems were used to synthesize both acoustic and visual speech. Decision trees with HMMs have been used to create expressive talking heads [3]. In [15], the Festival System was firstly used for speech synthesis followed by a text-to-visual-speech synthesis system and an audiovisual synchronizer. In [33], a learned phoneme-to-viseme mapping was also used for visual speech synthesis. Recently, many deep-learning-based

approaches have been proposed for visual speech synthesis. In [23], the authors used a unit-selection-based audiovisual speech synthesis system. In this approach, the output of a deep neural network (DNN) was used as a likelihood of each audiovisual unit in an inventory. Dynamic programming was then used to obtain the most likely trajectory of consecutive audiovisual units, which were later used for synthesis. A more neural based approach was proposed in [32], where a fully connected feed-forward neural network was used to synthesize natural-looking speech animation that is coherent with the input text and speech. In [20], an LSTM architecture was used to convert the input text into speech and corresponding coherent photo-realistic images of talking faces.

In contrast to these approaches, we use Tacotron2, a state-of-the-art architecture for acoustic speech synthesis, for synthesizing coherent acoustic and visual speech. The end-to-end approach described in this work synthesizes audiovisual speech in an end-to-end neural fashion using a single model.

Speech-driven Avatars: Voice Puppetry [5] is an early HMM-based approach for audio-driven facial animation. This was followed by techniques based on decision trees [19], or deep bidirectional LSTM [12] that outperformed HMM-based approaches. In [27], the authors proposed applying an LSTM-based neural network directly to audio features. In [31], a deep neural network was proposed to regress to a window of visual features from a sliding window of audio features. In this work, a time-shift recurrent network trained on an unlabeled visual speech dataset produced convincing results without having any dependencies on a speech recognition system. More recently, convolutional neural networks (CNNs) were used in [18] to learn a mapping from speech to the vertex coordinates of a 3D face model. Facial expressions and emotion were generated by a latent code extracted from the network. In [43], the authors propose VisemeNet which consisted of a three-stage LSTM network for lip sync. One stage predicts a sequence of phoneme-groups given the audio and another stage predicts the geometric location of landmarks given the audio. The final stage learns to use the predicted phoneme groups and facial landmarks to estimate parameters and sparse speech motion curves.

Most of these systems synthesize visual controllers that deform a 3D face model that looks like the speaker. In contrast, we predict a sequence of facial controllers that can be used across various fictional and human-like characters. For our modular approach, we use a CNN-based speech-to-animation model conditioned on emotion embeddings.

3 Estimation of the Ground Truth Blendshape Coefficients

One of the most challenging problems in facial animation is to find the ground-truth controllers of the face model. Manual labeling of the facial controls for each time frame in a dataset that is large enough to train a neural network is impractical, as annotation is both subjective, time consuming and expensive. Thus, ground truth facial controls are usually algorithmically estimated. In this study, we use an extension of the method described in [39] to automatically estimate the facial controls from RGB-D video streams.

We represent the space of facial expressions, including those caused by speech, using a low-dimensional generic blendshape model inspired by Ekman's Facial Action Coding System [11]. Such a model generates a mesh corresponding to a specific facial expression as

$$\mathbf{v}(\mathbf{x}) = \mathbf{b}_0 + \mathbf{B}\mathbf{x}, \tag{1}$$

where \mathbf{b}_0 is the neutral face mesh, the columns of matrix \mathbf{B} are additive displacements corresponding to a set of $n = 51$ blendshapes, and $\mathbf{x} \in [0, 1]$ are the weights applied to such blendshapes.

We construct a personalized model from a set of RGB-D sequences of fixed, predetermined prototypical expressions, such as neutral, mouth open, smile, anger, surprise, disgust and while the head is slightly rotating (these correspond to the matrix \mathbf{B} in the expression above) for the actor in our dataset. In particular, we use an extension of the example-based facial rigging method of [21], where we modify a generic blendshape model to best match the talent's example facial expressions. We improve registration accuracy over [21] by adding positional constraints to a set of 2D landmarks detected around the main facial features in the RGB images using a CNN similarly to [16].

Given the personalized model, we automatically generate labels for the head motion and blendshape coefficients (BSCs) by tracking every video frame of the subject. To do so, we rigidly align the

model to the depth maps using iterative closest point (ICP) with point-plane constraints. Then, we solve for the BSCs, which modify the model non-rigidly to best explain the input data. In particular, we use a point-to-plane fitting term on the depth map:

$$D_i(\mathbf{x}) = (\mathbf{n}_i^\top (\mathbf{v}_i(\mathbf{x}) - \bar{\mathbf{v}}_i))^2, \quad (2)$$

where \mathbf{v}_i is the i -th vertex of the mesh, $\bar{\mathbf{v}}_i$ is the projection of \mathbf{v}_i to the depth map, and \mathbf{n}_i is the surface normal of $\bar{\mathbf{v}}_i$. Additionally, we use a set of point-to-point fitting terms on the detected 2D facial landmarks:

$$L_j(\mathbf{x}) = \|\pi(\mathbf{v}_j(\mathbf{x})) - \mathbf{u}_j\|^2, \quad (3)$$

where \mathbf{u}_j is the position of a detected landmark and $\pi(\mathbf{v}_j(\mathbf{x}))$ is its corresponding mesh vertices projected into camera space. The terms D_i and L_j are combined in the following optimization problem:

$$\tilde{\mathbf{x}} = \underset{\mathbf{x}}{\operatorname{argmin}} \min w_d \sum_i D_i(\mathbf{x}) + w_l \sum_j L_j(\mathbf{x}) + w_r \|\mathbf{x}\|_1, \quad (4)$$

where w_d , w_l , and w_r represent the respective weights given to the depth term, the landmark term, and a L1 regularization term, which promotes the solution to be sparse. The minimization is carried out using a solver based on the Gauss-Seidel method. The estimated blendshape coefficients $\tilde{\mathbf{x}}$ in (4) are used as ground-truth facial controls for training the text-to-animation and audio-to-animation models in the subsequent sections.

4 Speech Emotion Features

Emotions in visual speech synthesis systems are increasingly required since they enhance the user experience and make the interaction more natural. Adding emotions to the synthesized acoustic and visual speech requires conditioning the neural network on some sort of a representation of the required emotion. In contrast to the style transfer approaches in [38] and [28] that have been recently successful in learning the speech style/emotion in an unsupervised manner, we chose to exploit emotion labels to train a separate neural network in a supervised way to classify emotions from speech. We consider the penultimate layer of the speech emotion classifier as a fine-grained vector representation of the emotion. Three basic emotion categories [24] are investigated in this paper: neutral, positive (happy) and negative (sad)

Figure 1 shows the architecture of the speech emotion classifier. In this approach, 40-dimensional mel-scaled filter bank speech features are firstly passed through a 1d-convolutional layer, which contains 100 filters with kernel size of 3×1 . The output of this convolutional layer is then fed into a single long short-term memory (LSTM) layer with 64 cells followed by a linear layer of the same dimension. A mean pooling layer is then used to summarize the LSTM outputs across time. A softmax layer is finally applied to the average pooling output to predict the emotion class.

After the model is trained, the output of the penultimate layer, i.e. the layer before the softmax layer, is used as the speech emotion embedding. These embeddings are used to condition the audiovisual speech synthesis systems during training as will be described in the upcoming sections. During inference, we use the speech emotion classifier to extract the emotion embedding from a reference utterance to get the desired emotion for the synthesized talking face. The audiovisual speech synthesizer is conditioned on that emotion embedding to synthesize speech and facial movements to match the emotion.

5 End-to-end Audiovisual Speech Synthesis

Deep neural networks, in particular sequence-to-sequence architectures [26, 37], has led to speech synthesizers producing almost human-like speech. Tacotron2 [26] is one of the most successful sequence-to-sequence architectures for speech synthesis. The Tacotron2 architecture takes as input a phoneme sequence of length M that represents the pronunciation of the sentence to be synthesized. As an output, Tacotron2 generates a sequence of 80-dimensional mel-scaled filter bank (MFB) features. The MFB features are finally used as an input to another sequence-to-sequence model, e.g., WaveRNN [17], to generate the samples of the synthesized speech signal.

In this paper, we adopt the Tacotron2 architecture for synthesizing not only the audio features, but also all 51 BSCs that control speech- and non-speech-related facial expressions.

Figure 1: Speech emotion recognition neural network. The network is trained to classify neutral, happy, and sad emotions using input acoustic features. Once the network is trained, the output of the average pooling layer is used as a speech emotion representation.

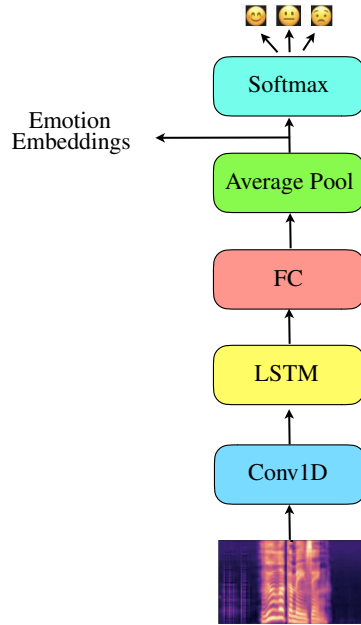


Figure 2: Tacotron2 architecture for emotional audiovisual speech synthesis. The network’s encoder converts an input sequence of phonemes and a compact representation of a predefined emotion into a sequence of abstract vector representations of the same length. An attention mechanism is used to focus on a subset of the encoded vectors at each time step. The concatenation of the weighted sum of the encoder outputs (the context vector) and a pre-processed regressor output vector are used as an input to the decoder. The decoder output is used to regress to visual and acoustic features that are finally post-processed to give a final cleaner features.

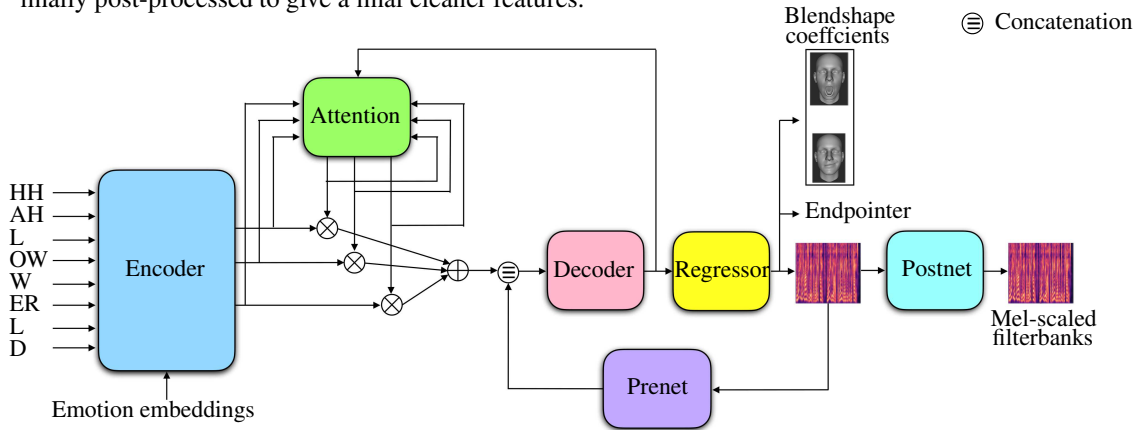
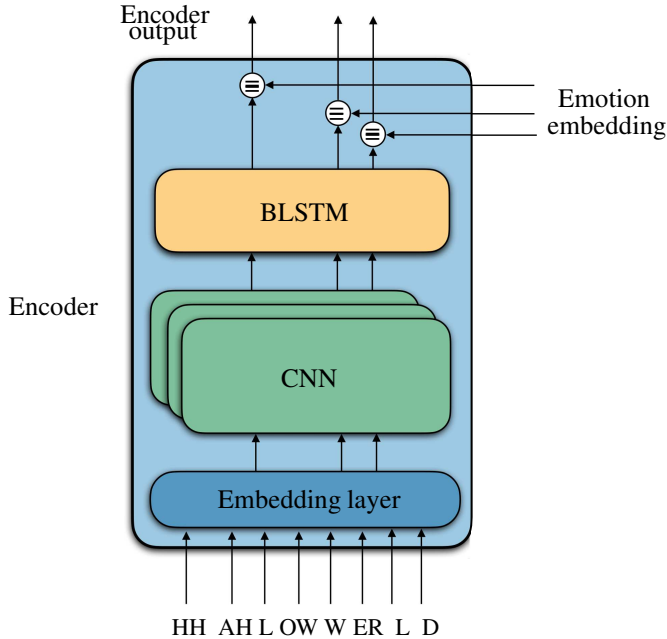


Figure 2 shows the entire architecture of AVTacotron2. Although the network is trained end-to-end, it can be divided into four major functional blocks: a phoneme encoder, an attention block, a decoder, and a regressor. In the following sections, these four blocks are described in detail.

5.1 Text Encoder

The function of the phoneme encoder in the Tacotron2 architecture is to transform a sequence of phonemes into an intermediate representation, from which acoustic and visual features can be generated. As shown in Figure 3, the input to the encoder is a sequence of M phoneme indices, which are transformed into 512-dimensional feature vectors using an embedding layer. As described in [26],

Figure 3: Emotion-conditioned phoneme encoder. The phoneme embeddings are processed by a set of convolution and bi-directional LSTM layers. The emotion embedding is repeated and cascaded with the processed phoneme embeddings to give the encoder outputs.



the $M \times 512$ output matrix of the embedding layers is passed through 3 convolutional layers, each of which has 512 feature maps with kernel size of 5×1 and ReLU activations. Each convolutional layer is followed by a drop-out layer with drop-out probability of 0.5 and batch normalization. The convolutional layers model the N-gram dependencies between consecutive phonemes [26]. For the longer term dependencies, the output of the final convolutional layer is processed by a bi-directional long short-term memory (BLSTM) layer with 512 units in each direction. The concatenation of the bi-directional LSTM gives the $M \times 1024$ intermediate representation of the M input phonemes. The 64 dimensional emotion embedding is repeated and cascaded with the processed phoneme embeddings to give the encoder outputs. During training the embeddings are extracted from the same output utterance. During inference, the emotion embedding is extracted from a reference utterance that has the required level of emotion. The emotionally conditioned phoneme representation is used to generate the audio-visual outputs in the later stages of the network, as will be described in the following sections.

5.2 Attention mechanism

A location-sensitive attention [8] is applied to the $M \times 1088$ phoneme intermediate representation that is output by the phoneme encoder. The output of the attention mechanism is called the context vector and is estimated as a weighted sum of the M intermediate representations. The attention and decoding blocks are applied in an iterative way. Therefore, the attention weights, i.e. alignments, of the t time-frames are determined by how much the intermediate representation is correlated with the decoder output of the $t - 1$ time-frame and to a processed version of the $t - 1$ estimated attention. The later gave rise to the name, location sensitive attention, where the processed alignments from the previous time frames help determine the decoder previous location and hence, motivates the model to process future frames without unreasonable loops or skips. The alignments of the previous time step is processed by a 1D convolutional layer of 32 feature maps, each of 31-dimensions. The correlation between the encoder output feature vectors, the decoder output of the previous time-frame, and the processed alignment of the previous time-frame is estimated using a weighted fully connected layer with tanh activations followed by a softmax layer for a normalization purpose as described in [26]. The context vector has 1088 dimensions and is used as the input to the decoder, which is the next stage of the network.

5.3 Decoder

The decoder stage of the Tacotron2 architecture is composed of two 1024-dimensional unidirectional LSTM layers. The decoder iteratively generates an embedding, from which all audio, video, and auxiliary information can be estimated. The input to the decoder at time-frame t are the context vector at time-frame t and a pre-processed version of the regressor output of the previous time-frame $t - 1$. Preprocessing of the regressor outputs is done by the so-called Pre-net, which is composed of two 256-dimensional fully-connected layers with ReLU activations. Since the decoder generates embeddings that are asynchronous with the encoder output, the number of output embeddings N_{decoder} is independent of the encoder output length M .

5.4 Regressor

The embeddings extracted from the decoder encodes all information needed to synthesize one or n acoustic and visual frames. We use $n = 2$ in this study, which means that the length of the synthesized acoustic and visual features is $2N_{\text{decoder}}$. The regressor is simply a linear projection of the embeddings from the decoder output onto the acoustic, the visual, and the auxiliary feature spaces. The acoustic feature space is the 80-dimensional MFBs. The visual feature space is the 51-dimensional BSCs. The auxiliary feature is a one-dimensional end-pointing feature that determines the end of decoding.

The output MFB features go through a post-processing network (post-net) that is composed of five 1D convolutional layers followed by a linear fully-connected layer. The convolutional layers have 512 filters of kernel size 5. The first four convolutional layers use (tanh) non-linear activations, whereas the final one has no non-linearity. A drop-out layer with drop-out probability of 0.5 is added after every convolutional layer. The final fully connected layer has 80 units, which is the same dimension as the regression acoustic feature space. A skip connection is added from the input of the post-net to its output, which means the post-net output represents the estimation residual. The residual is estimated with access to future frames, which makes the overall post-net output more accurate than the linearly projected MFB features.

The network is trained to minimize a weighted sum of four loss functions.

$$\mathcal{L}_{\text{total}} = \omega_{\text{mel}}\mathcal{L}_{\text{mel}} + \omega_{\text{post}}\mathcal{L}_{\text{post}} + \omega_{\text{end}}\mathcal{L}_{\text{end}} + \omega_{\text{bsc}}\mathcal{L}_{\text{bsc}}. \quad (5)$$

\mathcal{L}_{mel} is the L1 loss (mean absolute error) that is applied to the mel-scaled filter-bank features that are output from the linear projection layer. $\mathcal{L}_{\text{post}}$ and \mathcal{L}_{end} are the L2 (mean square error) losses that are applied to the output of the post-processing subnetwork and the end-pointing output respectively. For the BSCs, we use the L2 loss function \mathcal{L}_{bsc} . The weights ω_{mel} , ω_{post} , ω_{end} , and ω_{bsc} are empirically tuned to give the best synthesis performance. In our experiments, we use 0.9 for ω_{mel} , 1 for ω_{post} , 0.1 for ω_{end} and 0.9 for ω_{bsc} .

6 Modular Audiovisual Speech Synthesis

We adopt the Tacotron2 architecture in its standard audio-only version and feed the synthesized audio after reconstructing it from the predicted spectral features, e.g., using WaveRNN, into an audio-to-facial-animation module. On one hand, the AVTacotron2 system could give more accurate estimates of the lip movements since the embeddings extracted from the decoder are rich in acoustic and lexical information. On the other hand, the modular system is more flexible, as the audio-to-facial-animation network can be trained in a speaker-independent manner and used with any pre-trained text-to-speech voice. This would reduce the need for collecting hours of multimodal data for different speakers, which is necessary to train the AVTacotron2 model.

We have trained a CNN-based speaker-dependent audio-to-facial-animation neural network. The network architecture is shown in Table 1. The input acoustic features to the audio-to-facial-animation network is 40-dimensional filter bank features with a context window of 21 (10 past, current, and 10 future frames.) The acoustic features are extracted from the wav files. The acoustic speech synthesis is completely decoupled from the visual speech synthesis, so any text-to-speech system can be used. The ground truth BSCs described in Section 3 are used to train the network. The input to the penultimate fully connected layer is the concatenation of the former fully connected (FC) layer that encodes the audio features with the emotion embedding.

Table 1: The architecture of the audio-to-facial-animation network.

Type	#Filters	Kernel	Stride/padd.	Output	Act.
Conv.	128	3x3	1x1/same	21x40x128	RELU
Conv.	64	3x3	2x2/same	11x20x64	RELU
Conv.	64	3x3	1x1/same	11x20x64	RELU
Conv.	64	3x3	2x2/same	6x10x64	RELU
Conv.	64	3x3	1x1/valid	4x8x64	RELU
Conv.	64	3x3	1x1/valid	2x6x64	RELU
FC	512	-	-	1x1x512	RELU
FC+embed	128	-	-	1x1x128	RELU
FC	51	-	-	1x1x51	None

Table 2: The phoneme-viseme mapping used in our work and the viseme importance used to weight the loss of the audio-to-facial-animation-network. The weights are the normalized accuracy of an in-house video-based viseme classifier. The silence weight is heuristically set to zero.

Viseme cluster	Viseme	Phoneme	Weights
Bilabial	/P/	/p/ /b/ /m/	1.0
Labio-Dental	/F/	/f/ /v/	0.97
Palato alveolar	/SH/	/sh/ /zh/ /ch/ /jh/	0.75
Dental	/TH/	/th/ /dh/	0.66
Alveolar fricative	/Z/	/z/ /s/	0.66
Lip rounded vowels level 2	/V2/	/uw/ /uh/ /ow/ /w/	0.6
Lip rounded vowels level 1	/V1/	/aa/ /ah/ /ao/ /aw/ /er/ /oy/	0.59
Lip stretched vowels level 1	/V3/	/ae/ /eh/ /ey/ /ay /y/	0.58
Alveolar semivowels	/L/	/l/ /el/ /r/	0.5
Lip stretched vowels level 2	/V4/	/ih/ /iy/	0.48
Velar	/G/	/g/ /ng/ /k/ /hh/	0.46
Alveolar	/T/	/t/ /d/ /n/ /en/	0.36
Silence	/SIL/	/sil/ /sp/	0.0

In contrast to the end-to-end system, the audio-to-facial-animation network does not have access to the entire phoneme sequence. In order to compensate for that, the BSC loss \mathcal{L}_{bsc} in the audio-to-facial-animation network is modified. For each entry in a batch, the loss function is weighted differently. The weights of each entry are proportional to the importance of the corresponding spoken viseme (visual phoneme.) With these weights, the network is penalized more for inference errors related to important visemes, such as /p/ and /w/ and penalized less for errors related to less important visemes, such as /t/ and /g/. Table 2 shows the used viseme importance/weights, which are the classification accuracies of a video-based viseme classifier normalized over the maximum accuracy, which happens to be of the viseme /P/. The silence weight, which actually has the highest classification accuracy, is overridden and set to zero. Using these weights improves the performance of the audio-to-facial-animation network. We use a hybrid loss of L1 and the cosine distance (see [2]), which we found to be more effective than the L1 and L2 for small, sparse, and bounded labels, such as the BSCs. We have not used the hybrid loss in Equation 5, as the L2 was easier to balance with the other losses.

Table 3: Emotion classification performance from the Emotion Recognition System.

Emotion	Precision (%)	Recall (%)	F1-Score (%)
happy	95.0	96.0	96.0
sad	99.0	100.0	99.0
neutral	99.0	99.0	99.0
Accuracy (%)	97.8		

7 Experiments and Results

7.1 Dataset

A high quality multimodal corpus was collected for training all of our neural networks. The dataset consists of approximately 10 hours of multimodal data captured from a professional actress: 7 hours of neutral speech (~7270 sentences), 1.5 hours (~1430) of acted happy speech and 1.5 hours (~1430) of acted sad speech. In this dataset, there are 74 minutes (~300) common phrases spoken in a neutral, happy and sad emotional states. The text corpus was balanced to maintain a maximum phonetic coverage of US English phoneme-pairs. For each utterance in the corpus a single channel 44.1kHz audio, 60 frame per second (fps) 1920x1080 RGB video, and 30 fps depth signals were captured.

7.2 Experimental Setup and Results

7.2.1 Speech Emotion Recognition

For training the speech emotion recognition neural network, the corpus is randomly split into emotion-stratified partitions using a 80/20 rule. The resulting splits consist of 8116 utterances for training, 2029 utterances for validation, and 50 utterances for testing. As described in Section 4, 40-dimensional mel-scaled filter banks are used as input acoustic features. The network is trained to optimize a cross entropy loss using the Adam optimizer. We use a learning rate of 0.001 for a maximum of 20 epochs. We monitor the validation performance during training and apply early stopping when the validation loss converges. Since the data is class imbalanced, we penalize the classification errors of each class inversely proportional to the class probability.

Figure 4 shows a TSNE projection [35] of the emotion embeddings for the test set clustered based on emotion labels. As shown, the emotion embeddings are well separated, which is reflected in the high classification accuracy shown in Table 3. Although the performance of state-of-the-art speech emotion recognition systems in the wild does not reach such high accuracies [30], the high classification performance shown in Table 3 was actually expected, as the emotions are acted. In contrast to simply using a one hot vector to represent the emotion state, the distance between emotion embeddings within the same cluster allows for fine-grained control of the emotion level that needs to be synthesized.

7.2.2 Audiovisual Speech Synthesis

One of the most challenging tasks when it comes to machine learning problems involving synthesis is how to best compare models. Objective measures, such as the loss functions that the network is trained to optimize, do not usually reflect the naturalness and the quality of the network output. Human ratings of subjective quality are usually more reliable. In this study, we have conducted subjective tests to assess the quality of three different aspects of the synthesized talking face. The graders are gender balanced (15 male and 15 female) and they all are native US English speakers in the age range 2150.

Overall Experience of the Emotional Audiovisual Synthesis To assess the overall experience of the audiovisual emotional speech synthesis, we have conducted a subjective test, where graders are asked to evaluate videos from acoustic, visual, and overall naturalness perspectives. From the audio perspective, the graders are asked to evaluate the speech synthesis quality and emotion appropriateness given an emotion tag. To grade the visual aspects, the graders are asked to evaluate how much the visual synthesis (the synthesized lip movements and facial expressions) match the synthesized speech. Finally, the graders are asked to evaluate the overall naturalness of the talking face. Thirty

Figure 4: TSNE projection of the validation set emotion embeddings extracted using the speech emotion recognition system.

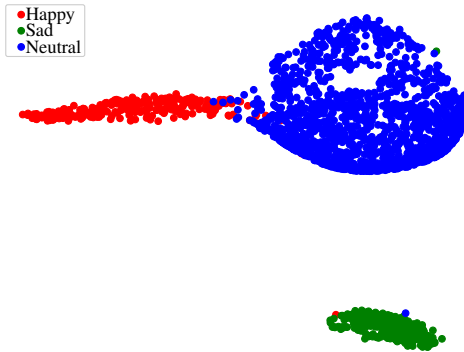



Figure 5: Grading template for the overall experience of the talking face

Instructions	<p>IMPORTANT: Please release the task if: * you do not have headphones, * there is background noise, * you have a hearing impairment, or * you can't hear/watch the audio/video samples for any reason It is important to understand that it is NOT you who is being tested - your results only provide information regarding the systems we are evaluating!</p> <p>Video Synthesis Evaluation We need your help evaluating video samples from an audio-visual speech synthesis system.</p>				
Video Label: happy					
Speech Synthesis Quality	Excellent	Good	Fair	Poor	Bad
Speech Emotion matches the given label	Perfectly	Most of the time	Sometimes	Doesn't match most of the time	Doesn't match at all
Lip movements follow speech	Perfectly	Most of the time	Sometimes	Doesn't follow most of the time	Doesn't follow at all
Facial Expression matches the emotion	Perfectly	Most of the time	Sometimes	Doesn't match most of the time	Doesn't match at all
How natural is the talking face overall?	Perfectly natural	Natural most of the time	Natural sometimes	Not natural most of the time	Not natural at all
Comments					

graders provided five mean opinion scores (MOSs) for the five questions described above. The scores range from (1) bad (no match) to (5) excellent (perfect match). Figure 5 shows the grading template used for evaluation.

We used 30 videos, half of which are synthesized with happy emotion and the other half with sad emotions. The MOS tests were conducted on each of the following sets of data - videos generated by the modular approach, videos generated by the end-to-end approach and the original(ground truth) recordings. We also used the acoustic speech synthesized from the end-to-end approach to drive the audio-to-facial-animation module in the modular approach to ensure fair comparison. In this way the graders hear the same speech with different lip movements from the two systems.

For all tests, the graders gave high scores (between good and excellent) as shown in Figures 6-10. All results are significant according to Mann-Whitney significance test. Figures 6-10 show that

Figure 6: Mean opinion scores comparing the quality of the lip movements synthesized by the end-to-end (E2E) and modular approaches to the ground truth (GT).

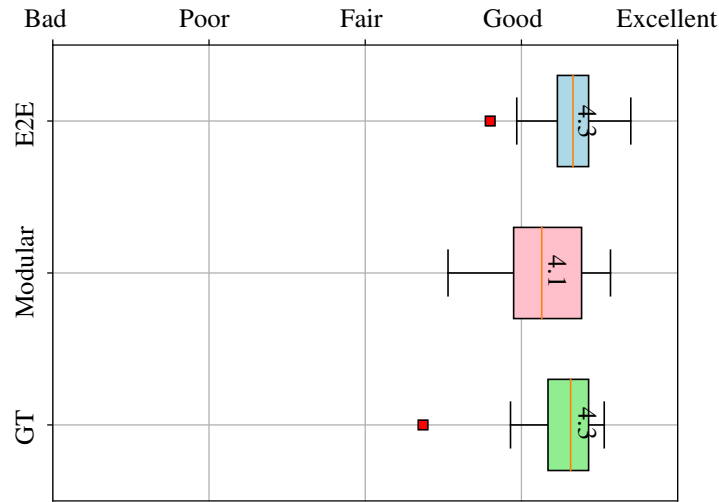
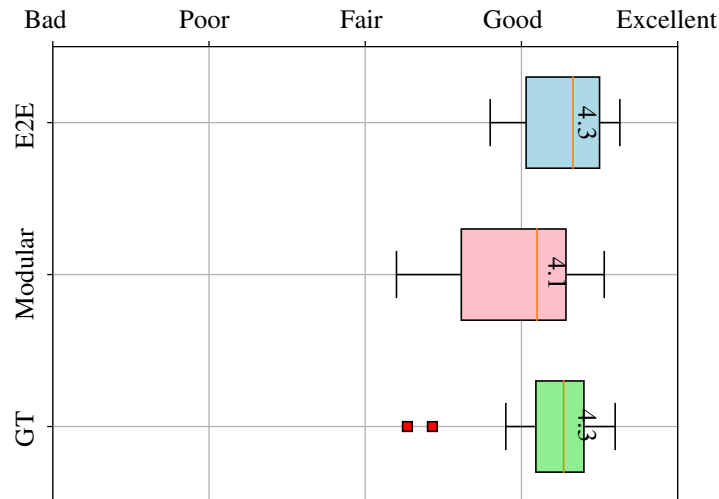


Figure 7: Mean opinion scores comparing the quality of the facial expressions synthesized by the end-to-end (E2E) and modular approaches to the ground truth (GT).



the end-to-end approach gives better and more consistent performance, i.e., small variance, than the modular approach in all aspects. Furthermore, the performance of the end-to-end approach is almost as good as the ground truth results. Figures 6-7 show results of grading the visual aspects of the synthesized talking face, i.e., lip movements and facial expressions. The ground truth results depicted in Figures 6-7 are also an indication of the performance of the offline blendshape estimation algorithms discussed in Section 3. The ground truth BSCs are estimated from RGB+depth images and the quality of these inputs relies on many factors, such as the head pose and lighting conditions. The outliers in the ground truth results in Figures 6, 7 and 12 are explained by cases where the BSC estimation may have failed when such conditions are not optimal. Neural networks on the other hand, when trained on these data, learn to filter out such outliers and infer the conditional mean. Therefore, the end-to-end approach shows a more consistent performance in Figures 6-7. In Figure 7, the larger variance of the modular approach synthesis is explained by the audio-to-animation model falling short in synthesizing reasonable emotional facial expressions from speech.

Figure 8: Mean opinion scores (MOS) comparing the synthesis quality of acoustic speech synthesized by the end-to-end (E2E) approach to the ground truth (GT). Visual aspects affect the MOS of the modular approach although same synthesized speech is used for both tests.

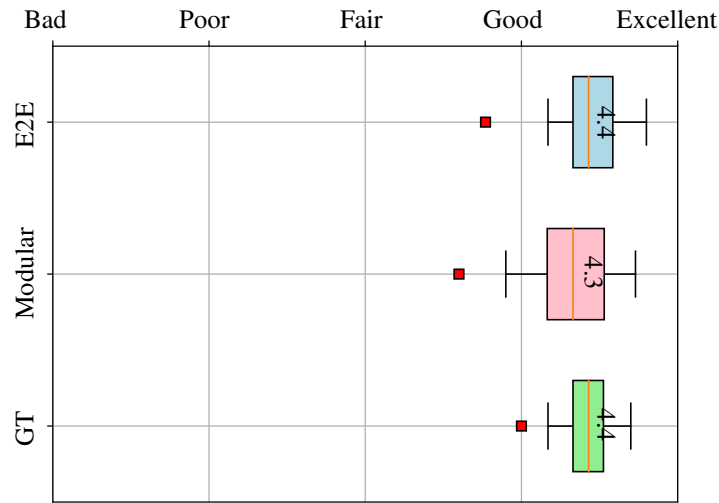
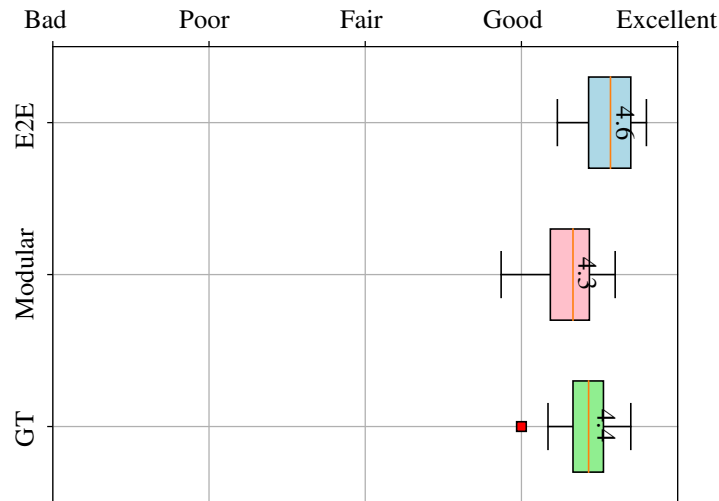


Figure 9: Mean opinion scores comparing the quality of the emotions in speech synthesized by the end-to-end (E2E) to the ground truth (GT). Visual aspects affect the MOS of the modular approach although same synthesized speech is used for both tests. Graders preferred the synthesized speech emotions which were more milder than the exaggerated acted emotions in the original recordings.



An interesting outcome from this study was that although the graders were instructed to completely ignore visual aspects when they grade the acoustic speech synthesis, the graders seemed to get unconsciously affected by the other aspects. This effect can be seen in the evaluation of the acoustic speech synthesis in Figures 8 and 9. Although, the speech synthesized from the end-to-end approach was the same speech used as input to the audio-to-animation model, the graders gave better speech synthesis and speech emotion scores to talking faces generated using the end-to-end approach.

Another interesting result is shown in Figure 9, where graders gave higher scores for the emotional speech synthesized from the end-to-end approach over the original recordings (GT). The reason for this is that in the original recording, the actor exaggerated happy and sad emotions in certain cases. We noticed that the emotions synthesized from the end-to-end approach are less exaggerated than the

Figure 10: Mean opinion scores comparing the quality of the holistic(overall) experience of the emotional talking faces synthesized by the end-to-end (E2E) and modular (Mod) approaches to the ground truth (GT).

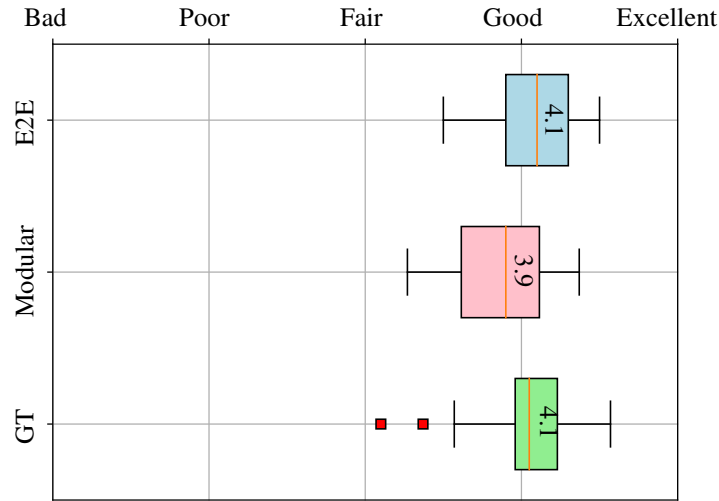
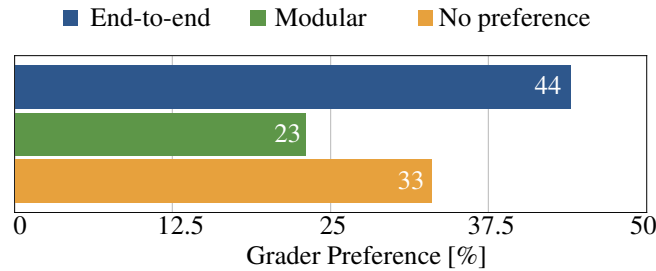


Figure 11: Results of the ABX test that comparing the quality of the avatar’s lip movements that are driven by the end-to-end and the modular approaches in an isolated setup.



original recordings. This effect is discussed more in the upcoming sections. The graders preferred less exaggerated happy and sad emotions in comparison to the overacted ones in the original dataset.

In order to evaluate the performance of the end-to-end and modular approaches in terms of acoustic and visual speech synthesis in a more independent manner, we introduce two additional subjective tests described in the subsequent sections that evaluate visual and acoustic speech synthesis performance isolated from all other aspects.

Visual Speech Synthesis We have conducted an AB test to compare the performance of the end-to-end approach and the modular approach in terms of the synthesized lip movements (visual speech), i.e. how naturally the avatar’s lip movements follow acoustic speech. In order for the graders to focus only on the quality of the synthesized visual speech, we have used a neutral emotion embedding to synthesize neutral speech. We have also eliminated (zeroed out) the controls of the upper half of the face, such as eyebrows movements and blinking. Human graders were given 50 pairs of videos that correspond to sentences that were not used during training. The graders were asked *which video matches the speech more naturally?* Graders were advised to focus only on the lip movements and to provide comments as to why they prefer their chosen video. To prevent display ordering effects, the order of the videos in a given pair is randomized. In total, 30 graders evaluated 50 videos.

Figure 11 shows that the graders preferred the performance of the end-to-end system more than the modular one. This result is significant according to Mann-Whitney significance test. The binary result of the AB test does not assess the *absolute* quality of the visual speech synthesized by any of the two approaches. To get an absolute quality score for each of the two systems, we have conducted two additional five point scale MOS tests for each approach individually using a similar setup of the AB test. The MOS test results depicted in Figure 12 shows that while the end-to-end approach is better than the modular approach, both systems generate very good lip movements.

Figure 12: Mean opinion scores of the visual speech synthesis of the end-to-end (E2E) and the modular (Mod) approaches in an isolated setup.

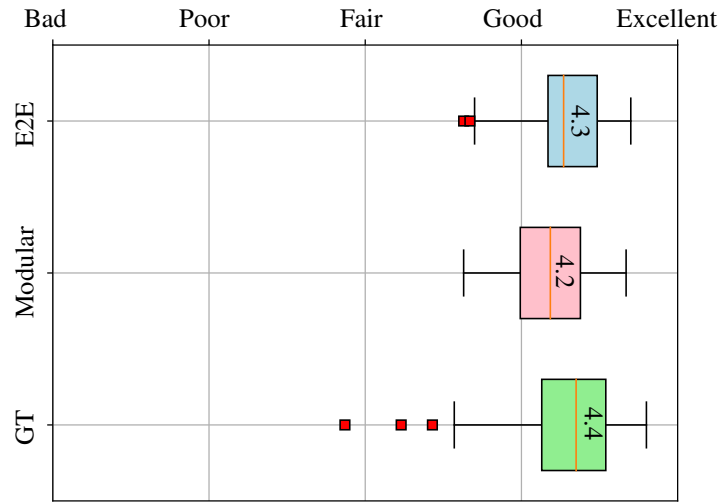
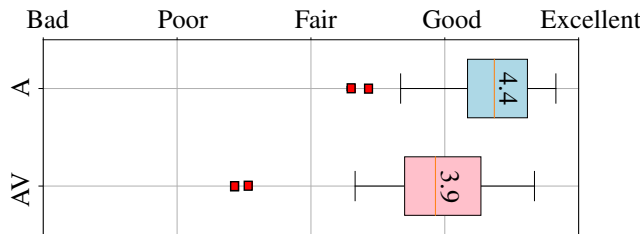


Figure 13: Mean opinion scores of the acoustic speech synthesis of the audiovisual (AV) and audio-only (A) synthesis systems that use Tacotron2 architecture.



7.2.2.3 Acoustic Speech Synthesis It is important to assess whether the quality of the synthesized acoustic speech is affected by adding the facial control estimation task to the Tacotron2 model. To assess this, we have conducted audio-only MOS tests for neutral speech, where graders were asked to primarily focus on assessing the quality of the synthesis. The graders were given 50 pairs of audio signals. Each pair consisted of a reference recording from the actor and a synthesized audio signal of the same phrase. The graders were asked to evaluate the synthesis quality given the reference signals on a five point scale, where one corresponds to poor quality and five to excellent quality. The MOS test was conducted one time with the audiovisual Tacotron2 and a second time with the conventional audio-only Tacotron2.

The results of the two MOS tests are shown in Figure 13. These results are significant according to Mann-Whitney significance test. Although the graders were explicitly instructed to focus only on the synthesis quality and not on the style of speech in the synthesized signal, the results and subsequent comments from the graders indicated that they were unconsciously affected by the speaking style. The low MOSs of the AVTacotron2 in Figure 13 is heavily weighted by the fact that the prosody of the synthesized speech does not always match the prosody of the reference signal. As shown in Figure 13, this was not the case in the traditional audio-only Tacotron2, where the prosody of the synthesis matches that of the reference signals and results in a higher MOS. The non-perfectly matching prosody is also the reason why the graders preferred milder emotional speech synthesis of AVTacotron2 than the overacted original recordings.

8 Conclusion

In this paper, we have described and compared two systems for audiovisual speech synthesis using Tacotron2. The first system is the AVTacotron2, which is an end-to-end system that takes an input text and synthesizes acoustic and visual speech. The second modular system uses the conventional audio-only Tacotron2 to synthesize acoustic speech from text. The synthesized speech is used as input to a speech-to-animation module that generates the corresponding facial controls. Emotion embeddings from a speech emotion classifier are used to allow both systems to synthesize emotional audiovisual speech. Both approaches are evaluated using a comprehensive subjective evaluation scheme. The results show that both systems produce synthesized talking faces that are almost as natural as the ground truth ones. Both approaches generate production-quality speech and facial animation that can be applied to a variety of fictional and human-like face models without post-processing. The end-to-end approach outperforms the modular approach in almost all aspects. However, the additional task of the facial control estimation in the end-to-end approach can sometimes lead to a mismatch between the prosody of the synthesized acoustic speech and the original recordings.

In order to enhance the experience of the talking faces, our on-going work involves the task of estimating head pose in addition to lip movements and facial expression. We are currently investigating the impact of the hybrid loss function on AVTacotron2 and estimating optimal weighting factors for audio and visual losses. We are also working on improving the prosody of the synthesized acoustic speech from the AVTacotron2. Finally, we are investigating video-based and audiovisual-based emotion embeddings compared to the audio-only one used here.

9 Acknowledgments

The authors are grateful to Oggi Rudovic, Barry-John Theobald, and Javier Latorre Martinez for their valuable comments.

References

- [1] A. Abdelaziz, B. Theobald, J. Binder, G. Fanelli, P. Dixon, N. Apostoloff, T. Weise, and S. Kajari. Speaker-independent speech-driven visual speech synthesis using domain-adapted acoustic models. In *International Conference on Multimodal Interaction*, pages 220–225, 2019.
- [2] Zakaria Aldeneh, Anushree Prasanna Kumar, Barry-John Theobald, Erik Marchi, Sachin Kajari, Devang Naik, and Ahmed Hussen Abdelaziz. Self-supervised learning of visual speech features with audiovisual speech enhancement. *arXiv preprint arXiv:2004.12031*, 2020.
- [3] Robert Anderson, Björn Stenger, Vincent Wan, and Roberto Cipolla. An expressive text-driven 3d talking head. In *ACM SIGGRAPH 2013 Posters*, pages 1–1. 2013.
- [4] Thabo Beeler, Fabian Hahn, Derek Bradley, Bernd Bickel, Paul Beardsley, Craig Gotsman, Robert W Sumner, and Markus Gross. High-quality passive facial performance capture using anchor frames. In *ACM SIGGRAPH 2011 papers*, pages 1–10. 2011.
- [5] M. Brand. Voice puppetry. In *Proceedings of the 26th annual conference on Computer graphics and interactive techniques*, pages 21–28. ACM Press/Addison-Wesley Publishing Co., 1999.
- [6] Chen Cao, Derek Bradley, Kun Zhou, and Thabo Beeler. Real-time high-fidelity facial performance capture. *ACM Transactions on Graphics (ToG)*, 34(4):1–9, 2015.
- [7] Chen Cao, Hongzhi Wu, Yanlin Weng, Tianjia Shao, and Kun Zhou. Real-time facial animation with image-based dynamic avatars. *ACM Transactions on Graphics*, 35(4), 2016.
- [8] Jan K Chorowski, Dzmitry Bahdanau, Dmitriy Serdyuk, Kyunghyun Cho, and Yoshua Bengio. Attention-based models for speech recognition. In *Advances in neural information processing systems*, pages 577–585, 2015.
- [9] Timothy F. Cootes, Gareth J. Edwards, and Christopher J. Taylor. Active appearance models. *IEEE Transactions on pattern analysis and machine intelligence*, 23(6):681–685, 2001.

- [10] Jack Chilton Cotton. Normal visual hearing. *Science*, 1935.
- [11] P. Ekman and W. Friesen. *Facial Action Coding System: A Technique for the Measurement of Facial Movement*. Consulting Psychologists Press, Palo Alto, 1978.
- [12] B. Fan, L. Wang, F. Soong, and L. Xie. Photo-real talking head with deep bidirectional LSTM. In *IEEE International Conference on Acoustics, Speech and Signal Processing (ICASSP)*, pages 4884–4888. IEEE, 2015.
- [13] S. Fu, R. Gutierrez-Osuna, A. Esposito, P. Kakumanu, and O. Garcia. Audio/visual mapping with cross-modal hidden Markov models. *IEEE Transactions on Multimedia*, 7(2):243–252, 2005.
- [14] Graham Fyffe, Andrew Jones, Oleg Alexander, Ryosuke Ichikari, Paul Graham, Koki Nagano, Jay Busch, and Paul Debevec. Driving high-resolution facial blendshapes with video performance capture. In *ACM SIGGRAPH 2013 Talks*, pages 1–1. 2013.
- [15] Udit Kumar Goyal, Ashish Kapoor, and Prem Kalra. Text-to-audiovisual speech synthesizer. In *International Conference on Virtual Worlds*, pages 256–269. Springer, 2000.
- [16] Zhenliang H., Meina K., Jie J., Xilin C., and Shiguang S. A fully end-to-end cascaded CNN for facial landmark detection. In *IEEE International Conference on Automatic Face & Gesture Recognition*, pages 200–207, 2017.
- [17] Nal Kalchbrenner, Erich Elsen, Karen Simonyan, Seb Noury, Norman Casagrande, Edward Lockhart, Florian Stimberg, Aaron van den Oord, Sander Dieleman, and Koray Kavukcuoglu. Efficient neural audio synthesis. *arXiv preprint arXiv:1802.08435*, 2018.
- [18] T. Karras, T. Aila, S. Laine, A. Herva, and J. Lehtinen. Audio-driven facial animation by joint end-to-end learning of pose and emotion. *ACM Transactions on Graphics (TOG)*, 36(4):94, 2017.
- [19] T. Kim, Y. Yue, S. Taylor, and I. Matthews. A decision tree framework for spatiotemporal sequence prediction. In *Proceedings of the 21th ACM SIGKDD International Conference on Knowledge Discovery and Data Mining*, pages 577–586. ACM, 2015.
- [20] Rithesh Kumar, Jose Sotelo, Kundan Kumar, Alexandre de Brébisson, and Yoshua Bengio. Obamanet: Photo-realistic lip-sync from text. *arXiv preprint arXiv:1801.01442*, 2017.
- [21] H. Li, T. Weise, and M. Pauly. Example-based facial rigging. In *ACM SIGGRAPH*, pages 32:1–32:6. ACM, 2010.
- [22] Harry McGurk and John MacDonald. Hearing lips and seeing voices. *Nature*, 264(5588):746–748, 1976.
- [23] Jonathan Parker, Ranniery Maia, Yannis Stylianou, and Roberto Cipolla. Expressive visual text to speech and expression adaptation using deep neural networks. In *2017 IEEE International Conference on Acoustics, Speech and Signal Processing (ICASSP)*, pages 4920–4924. IEEE, 2017.
- [24] John Sabini and Maury Silver. Ekman’s basic emotions: Why not love and jealousy? *Cognition & Emotion*, 19(5):693–712, 2005.
- [25] Shinji Sako, Keiichi Tokuda, Takashi Masuko, Takao Kobayashi, and Tadashi Kitamura. HMM-based text-to-audio-visual speech synthesis. In *Sixth International Conference on Spoken Language Processing*, 2000.
- [26] Jonathan Shen, Ruoming Pang, Ron J Weiss, Mike Schuster, Navdeep Jaitly, Zongheng Yang, Zhifeng Chen, Yu Zhang, Yuxuan Wang, Rj Skerrv-Ryan, et al. Natural TTS synthesis by conditioning WAVENet on mel spectrogram predictions. In *2018 IEEE International Conference on Acoustics, Speech and Signal Processing (ICASSP)*, pages 4779–4783. IEEE, 2018.
- [27] T. Shimba, R. Sakurai, H. Yamazoe, and J. Lee. Talking heads synthesis from audio with deep neural networks. In *2015 IEEE/SICE International Symposium on System Integration (SII)*, pages 100–105. IEEE, 2015.

- [28] RJ Skerry-Ryan, Eric Battenberg, Ying Xiao, Yuxuan Wang, Daisy Stanton, Joel Shor, Ron J Weiss, Rob Clark, and Rif A Saurous. Towards end-to-end prosody transfer for expressive speech synthesis with Tacotron. *arXiv preprint arXiv:1803.09047*, 2018.
- [29] Linsen Song, Wayne Wu, Chen Qian, Chen Qian, and Chen Change Loy. Everybodys talkin: Let me talk as you want. *arXiv preprint*, arXiv:, 2020.
- [30] Lorenzo Tarantino, Philip N Garner, and Alexandros Lazaridis. Self-attention for speech emotion recognition. *Proc. Interspeech 2019*, pages 2578–2582, 2019.
- [31] S. Taylor, A. Kato, B. Milner, and I. Matthews. Audio-to-visual speech conversion using deep neural networks. In *Interspeech*. International Speech Communication Association, 2016.
- [32] S. Taylor, T. Kim, Y. Yue, M. Mahler, J. Krahe, A. Rodriguez, J. Hodgins, and I. Matthews. A deep learning approach for generalized speech animation. *ACM Transactions on Graphics (TOG)*, 36(4):93, 2017.
- [33] S. Taylor, M. Mahler, B. Theobald, and I. Matthews. Dynamic units of visual speech. In *Proceedings of the ACM SIGGRAPH/Eurographics Symposium on Computer Animation*, pages 275–284. Eurographics Association, 2012.
- [34] Justus Thies, Mohamed Elgharib, Ayush Tewari, Christian Theobald, and Matthias Nießner. Neural voice puppetry: Audio-driven facial reenactment. *arXiv 2019*, 2019.
- [35] Laurens van der Maaten and Geoffrey Hinton. Visualizing data using t-SNE. *journal of machine learning research* 9. *Nov (2008)*, 2008.
- [36] Lijuan Wang, Xiaojun Qian, Lei Ma, Yao Qian, Yining Chen, and Frank K Soong. A real-time text to audio-visual speech synthesis system. In *Ninth Annual Conference of the International Speech Communication Association*, 2008.
- [37] Yuxuan Wang, RJ Skerry-Ryan, Daisy Stanton, Yonghui Wu, Ron J Weiss, Navdeep Jaitly, Zongheng Yang, Ying Xiao, Zhifeng Chen, Samy Bengio, et al. Tacotron: Towards end-to-end speech synthesis. *arXiv preprint arXiv:1703.10135*, 2017.
- [38] Yuxuan Wang, Daisy Stanton, Yu Zhang, RJ Skerry-Ryan, Eric Battenberg, Joel Shor, Ying Xiao, Fei Ren, Ye Jia, and Rif A Saurous. Style tokens: Unsupervised style modeling, control and transfer in end-to-end speech synthesis. *arXiv preprint arXiv:1803.09017*, 2018.
- [39] T. Weise, S. Bouaziz, H. Li, and M. Pauly. Realtime performance-based facial animation. In *ACM transactions on graphics (TOG)*, volume 30, page 77. ACM, 2011.
- [40] Yanlin Weng, Chen Cao, Qiming Hou, and Kun Zhou. Real-time facial animation on mobile devices. *Graphical Models*, 76(3):172–179, 2014.
- [41] L. Xie and Z. Liu. Realistic mouth-synching for speech-driven talking face using articulatory modelling. *IEEE Transactions on Multimedia*, 9(3):500–510, 2007.
- [42] Li Zhang, Noah Snavely, Brian Curless, and Steven M Seitz. Spacetime faces: High-resolution capture for modeling and animation. In *Data-Driven 3D Facial Animation*, pages 248–276. Springer, 2008.
- [43] Yang Zhou, Zhan Xu, Chris Landreth, Evangelos Kalogerakis, Subhransu Maji, and Karan Singh. Visemenet: Audio-driven animator-centric speech animation. *ACM Transactions on Graphics (TOG)*, 37(4):1–10, 2018.